(t,x) domain, pattern-based ground roll removal

Morgan Brown and Robert G. Clapp, Stanford University*

SUMMARY

We demonstrate the use of a new, $t-x$ domain, pattern-based signal/noise separation technique to separate ground roll from primary reflection events. Ground roll is notoriously difficult to model with generality, but the technique requires a kinematically correct model of the noise. We obtain an imperfect model of the ground roll directly from the data itself, by application of a suitable lowpass filter. On a 2-D receiver line gather taken from a 3-D shot gather, in which the ground roll is spatially aliased and has nonlinear moveout, the separation results improve markedly over direct subtraction of the noise model from the data.

INTRODUCTION

In many terrestrial environments, high-amplitude ground roll – to first order direct-arrival and scattered energy from the shot-generated Rayleigh (SV) wave – is the main impediment to seismic imaging. Since they depend on the highly variable earth properties of the near surface, the kinematics of surface waves is difficult to model, particularly if the scattered wavefield is strong. In (t,x,y) space, the ground roll falls within a cone centered at the shot location, and is spatially aliased at normal receiver spacing. A single 2-D receiver line gather from a 3-D cross-spread geometry shot gather is shown in Figure 1. In many practical situations, the "ground roll

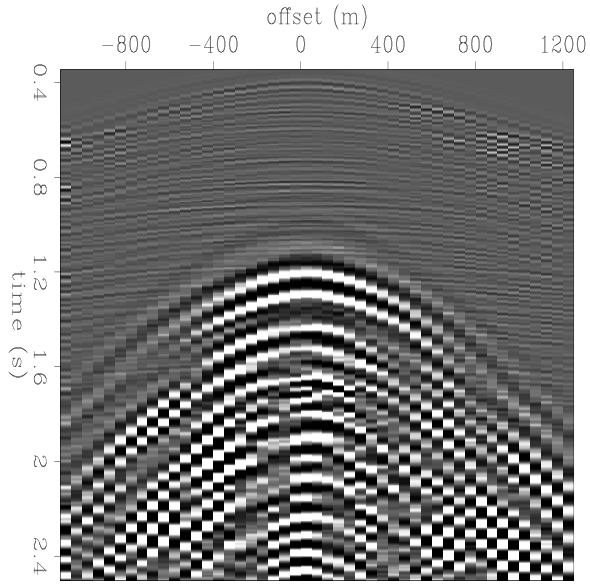

Figure 1: Left: Receiver line windowed from a 3-D shot gather of a Middle East cross-spread survey. The penetration depth of Rayleigh waves is a decreasing function of frequency, so they are dispersive if the near surface has a heterogeneous velocity profile. Aliased, dispersive ground roll with non-linear moveout overpowers reflection events in the lower portion of the section.

cone" is simply muted from prestack data. While this practice may often give a kinematically-correct image, some applications, like multicomponent seismic and quantitative inversion, require both near and far offsets. Moreover, for deep targets, recording far-enough offsets may prove cost prohibitive.

Field array stacks always blur the recorded wavelet somewhat, since incident primary reflections are never perfectly vertical and the near surface is laterally variant. Furthermore, as with Ocean Bottom Cable (OBC) applications, placement of arrays with adequate areal extent may be logistically impossible. Finally, traditional 2-D field arrays are ineffective at removing out-of-plane backscattered energy, so a 3-D array is required to suppress it (Regone, 1997), adding considerably to the acquisition cost.

Ground roll normally occupies a lower temporal frequency band than reflection events (see Fig. 2), in which case the former is removable by a simple highpass filtering operation, at the expense of the low frequency components of the reflections. $f-k$ filtering is useful for removing linear events, but the process is sensitive to spatially aliased data and is prone to Gibbs-like truncation artifacts. In 3-D, the aliasing becomes even more pronounced, since high land seismic acquisition costs usually prevent adequate sampling of the crossline axis.

Pattern-based signal/noise separation techniques do not impose any prior assumptions regarding the moveout of the data – the only thing required is a kinematically-correct model of the noise to be removed. Recent approaches for multiple suppression (Spitz, 1999; Bednar and Neale, 1999) operate in the $f-x$ domain, balancing a definite speed advantage over $t-x$ domain techniques with the limiting assumption that the data be time-stationary. Since ground roll is often highly dispersive, and thus temporally nonstationary, a $t-x$ domain approach is a more appropriate choice for ground roll removal.

METHODOLOGY

Consider the recorded data to be the simple superposition of "signal", i.e., reflection events and "noise", i.e., ground roll: $\mathbf{d}=\mathbf{s}+\mathbf{n}$. For the special case of uncorrelated signal and noise, the so-called *Wiener estimator* is a filter, which when applied to the data, yields an optimal (least-squares sense) estimate of the embedded signal (Castleman, 1996). The frequency response of this filter is

$$\mathbf{H}=\frac{\mathbf{P_s}}{\mathbf{P_n}+\mathbf{P_s}}, \tag{1}$$

where $\mathbf{P_s}$ and $\mathbf{P_n}$ are the signal and noise power spectra, respectively. Abma (1995) and Claerbout (1998a) solved a constrained least squares problem to separate signal from spatially uncorrelated noise:

$$\begin{aligned} \mathbf{Nn} &\approx 0 \\ \epsilon\mathbf{Ss} &\approx 0 \\ \text{subject to} &\leftrightarrow \mathbf{d}=\mathbf{s}+\mathbf{n} \end{aligned} \tag{2}$$

where the operators $\mathbf{N}$ and $\mathbf{S}$ represent $t-x$ domain convolution with nonstationary Prediction Error filters (PEF's) which whiten the unknown noise $\mathbf{n}$ and signal $\mathbf{s}$, respectively. ϵ is a Lagrange multiplier. Minimizing the quadratic objective function suggested by equation (2) with respect to $\mathbf{s}$ leads to the following expression for the estimated signal:

$$\hat{\mathbf{s}}=\left(\mathbf{N^T N}+\epsilon^2\mathbf{S^T S}\right)^{-1}\mathbf{N^T N}\,\mathbf{d} \tag{3}$$

By construction, the frequency response of a PEF approximates the inverse power spectrum of the data from which it was estimated. Thus we see that the approach of equation (2) is similar to the Wiener reconstruction process.

A suitable noise model must contain the basic spatial correlation of all noise events but may differ from the actual noise by an arbitrary nonstationary scale factor. Figure 2 shows the average temporal power spectrum of the 2-D receiver line gather of Figure 1 and the interpreted signal and noise spectra. We exploit the separation in temporal frequency and model the ground roll by applying a 15 Hz lowpass filter to the data. Although the noise model will generally be spatially aliased like the data, Crawley (1998) showed that $t-x$ domain nonstationary PEF's can be estimated safely from spatially aliased data.

Spitz (1999) showed that for uncorrelated signal and noise, the signal PEF can be expressed in terms of a PEF, **D**, estimated from the *data* **d**, and a PEF, **N**, estimated from the noise model:

$$\mathbf{S} = \mathbf{D}\mathbf{N}^{-1} \tag{4}$$

Spitz' result applies to one-dimensional PEF's in the $f-x$ domain, but our use of the Helix transform (Claerbout, 1998b) permits stable inverse filtering with multidimensional $t-x$ domain filters.

Substituting $\mathbf{S} = \mathbf{D}\mathbf{N}^{-1}$ and applying the constraint $\mathbf{d} = \mathbf{s} + \mathbf{n}$ to equation (2) gives

$$\begin{aligned} \mathbf{N}\mathbf{s} &\approx \mathbf{N}\mathbf{d} \\ \epsilon\mathbf{D}\mathbf{N}^{-1}\mathbf{s} &\approx \mathbf{0}. \end{aligned} \tag{5}$$

Iterative solutions to least-squares problems converge faster if the data and the model being estimated are both uncorrelated. To precondition this problem, we again appeal to the Helix transform to make the change of variables $\mathbf{x} = \mathbf{S}\mathbf{s} = \mathbf{D}\mathbf{N}^{-1}\mathbf{s}$ or $\mathbf{s} = \mathbf{N}\mathbf{D}^{-1}\mathbf{x}$ and apply it to equation (5):

$$\begin{aligned} \mathbf{N}\mathbf{N}\mathbf{D}^{-1}\mathbf{x} &\approx \mathbf{N}\mathbf{d} \\ \epsilon\mathbf{x} &\approx \mathbf{0} \end{aligned} \tag{6}$$

After solving equation (6) for the preconditioned solution **x**, we obtain the estimated signal by reversing the change of variables: $\hat{\mathbf{s}} = \mathbf{N}\mathbf{D}^{-1}\mathbf{x}$.

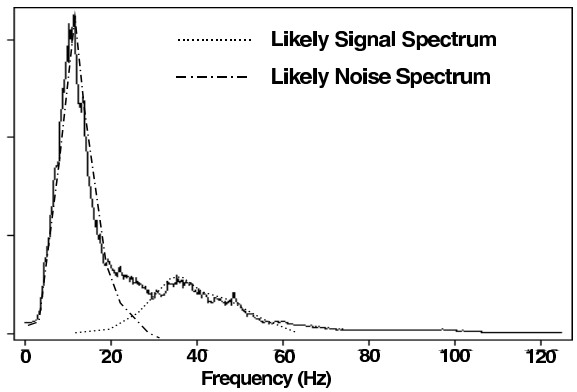

Figure 2: Solid line - Average amplitude spectrum of 2-D gather shown in Figure 1. Dotted line - interpreted signal spectrum. Dashed line - interpreted noise spectrum.

RESULTS

The result of applying the technique to the 2-D receiver line (Fig. 1) is shown in Figures 5 and 6. Turn the page on its side to properly view the data. We display each half of the gather separately, to better facilitate direct comparison. The "Model" panel of Figure 5 shows the shows the left half of the noise model - simply a 15 Hz lowpass filter applied to the data - and the direct subtraction of this noise model from the data. Clearly, direct subtraction - effectively highpass filtering - does not satisfactorily suppress the ground roll. The "Estimated" panel of Figure 5 shows the the left half (flipped left-to-right) of the estimated noise and the estimated signal, both obtained by application of the $t-x$ domain pattern-based separation algorithm. Figure 6 is the analogous plot for the right hand side of the gather in Figure 1, but in this case, it is the noise model which is flipped left-to-right.

Although the separation is clearly still incomplete, the results are worthy of note for several reasons. According to our interpetation (Fig. 2), we expect direct subtraction to be imperfect because the 15 Hz lowpass filter used to create the noise model will not include higher frequency components of the ground roll, in order to avoid removing too much signal. However, from Figures 5 and 6, notice that the pattern-based separation technique effectively and nondestructively separates much of this "overlapping" noise from the underlying signal, particularly for the aliased events at far offsets.

Figures 3 and 4 examine the results closely, on a 100-by-9 window of data. Notice that a 15 Hz-cutoff lowpass filter applied to the data appears to consist almost exclusively of noise, while a 30 Hz-cutoff highpass filter is nearly all signal. From the spectra, we see that the energy levels of the modeled noise and signal are markedly lower than that of the data. Visually, we notice that the estimated signal and noise panels produced by the pattern-based separation technique have the same character as their respective models, but the energy level now matches the data, according to the corresponding spectral plot. The separation has correctly meted out signal and noise energy in the overlapping 15-30 Hz band. Notice that a small amount of signal appears to have crept into the noise panel, and the corresponding energy in the estimated noise spectrum at high frequencies. The parameter ϵ in equation (6) (roughly an estimate of the noise-to-signal ratio) controls the amount of "noise" removed from the data. Since the noise-to-signal ratio of real land data normally varies considerably throughout the section, the task of choosing ϵ always entails a compromise.

CONCLUSIONS

We applied a $t-x$ domain, pattern-based signal/noise separation algorithm to a 2-D receiver line gather contaminated with spatially aliased, nonlinear-moveout ground roll. To obtain a kinematic model of the noise, we exploited the fact that ground roll is generally first-order separable from the underlying signal by lowpass filtering. In spite of spatial aliasing, and an imperfect noise model (insofar as direct subtraction gave an unsatisfactory result), the data was well-separated into estimated signal and noise panels. The specific moveout properties of the ground roll were not taken into account. Parenthetically, note that the methodology applied here is better termed *wavefield separation*. A robust estimate of the wave modes making up ground roll may provide a wealth of information about the earth properties of the near surface zone.

ACKNOWLEDGEMENTS

Sergey Fomel wrote much of the core nonstationary filtering code used for this algorithm. Professor Kurt Marfurt of Allied Geophysical Laboratory provided helpful advice during a visit to SEP.

REFERENCES

Abma, R., 1995, Least-squares separation of signal and noise with multidimensional filters: Ph.D. thesis, Stanford University.

Bednar, J. B., and Neale, G. H., 1999, A comparison of pattern and series based multiple suppression: 69th Annual Internat. Mtg., Soc. Expl. Geophys., Expanded Abstracts, pages 1056–1059.

Castleman, K. R., 1996, Digital image processing: Prentice-Hall.

Claerbout, J. Geophysical estimation by example: Environmental soundings image enhancement:. http://sepwww.stanford.edu/sep/prof/, 1998.

Claerbout, J., 1998b, Multidimensional recursive filters via a helix: Geophysics, **63**, no. 5, 1532–1541.

Crawley, S. E., 1998, Shot interpolation for radon multiple suppression: 68th Annual Internat. Mtg., Soc. Expl. Geophys., Expanded Abstracts, pages 1238–1241.

Regone, C. J., 1997, Measurement and identification of 3-d coherent noise generated from irregular surface carbonates, *in* Marfurt, K. J., Ed., Carbonate seismology: Soc. Expl. Geophys., 281–305.

Spitz, S., 1999, Pattern recognition, spatial predictability, and subtraction of multiple events: The Leading Edge, **18**, no. 1, 55–58.

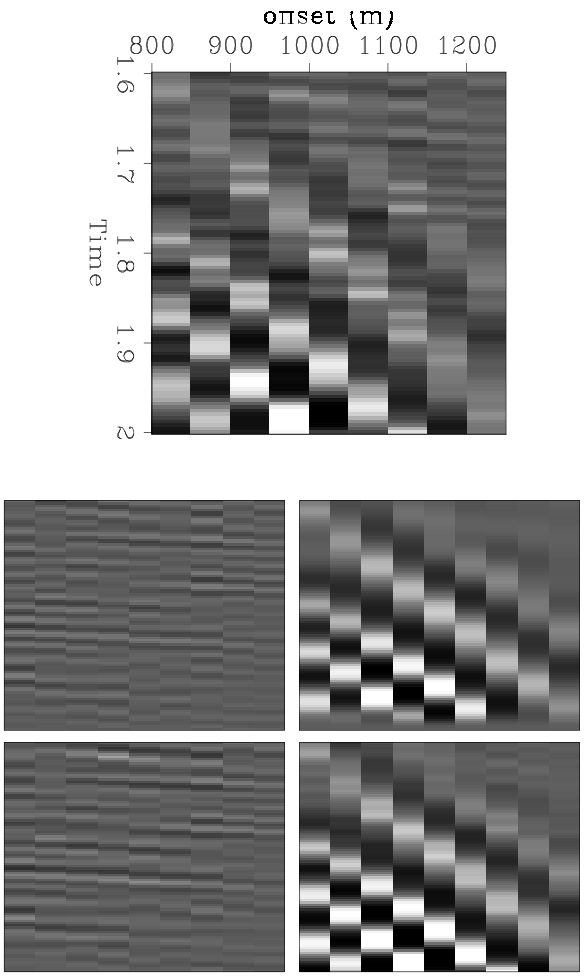

Figure 3: Top: Small window taken directly from gather of Figure 1. Middle: Model of primary reflections (highpass filter with 30 Hz cutoff) and model of noise (lowpass filter with 15 Hz cutoff). Bottom: Pattern-based estimate of primary reflections and noise.

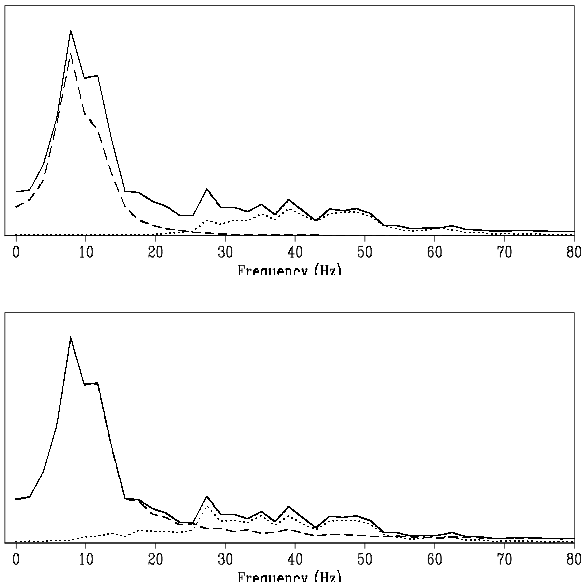

Figure 4: Refer to Figure 3. Top: Solid line - average temporal spectrum of data window; Dotted line - spectrum of modeled primary reflections; Dashed line - spectrum of modeled noise. Bottom: Solid line - average temporal spectrum of data window; Dotted line - spectrum of pattern-based-estimated primary reflections; Dashed line - spectrum of estimated noise.

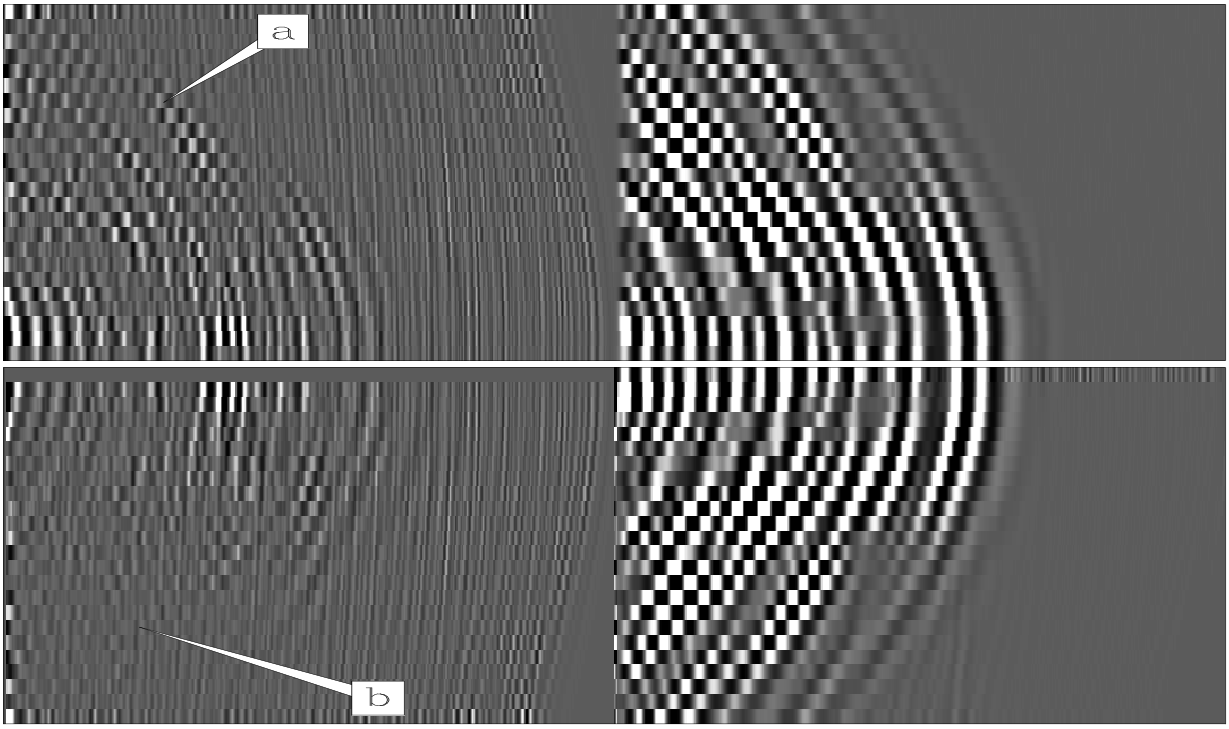

Figure 5: Left half of 2-D gather (Fig. 1). “Model” panel: Noise model and noise model directly subtracted from data. “Estimated” panel: Pattern-based estimated noise and estimated signal. (a) shows aliased noise not removed by direct substraction. (b) shows “hidden” primary reflection uncovered by separation.

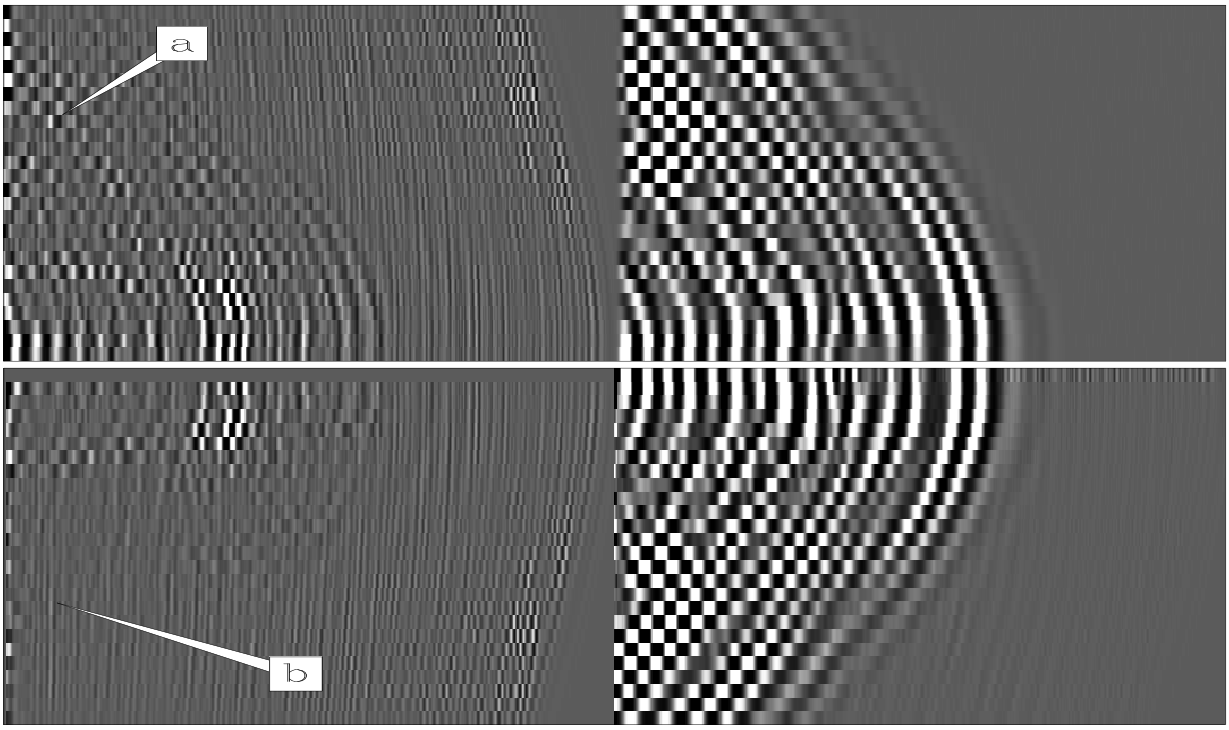

Figure 6: Right half of 2-D gather (Fig. 1). “Model” panel: Noise model and noise model directly subtracted from data. “Estimated” panel: Pattern-based estimated noise and estimated signal. (a) shows aliased noise not removed by direct substraction. (b) shows “hidden” primary reflection uncovered by separation.